Resolution of d'Alembert's Paradox

Johan Hoffman* and Claes Johnson*

May 20, 2008

Abstract

We propose a resolution of d'Alembert's Paradox comparing observation of substantial drag/lift in fluids with very small viscosity such as air and water, with the mathematical prediction of zero drag/lift of stationary irrotational solutions of the incompressible inviscid Euler equations, referred to as potential flow. We present analytical and computational evidence that (i) potential flow cannot be observed because it is illposed or unstable to perturbations, (ii) computed viscosity solutions of the Euler equations with slip boundary conditions initiated as potential flow, develop into turbulent solutions which are wellposed with respect to drag/lift and which show substantial drag/lift, in accordance with observations.

Keywords: d'Alembert's Paradox, Euler equations, inviscid flow, General Galerkin method, illposed, wellposed, separation, blowup.

AMS subject classification: 65M60, 76E99

How wonderful that we have met with a paradox. Now we have some hope of making progress. (Nils Bohr)

1 Introduction

We propose a resolution of *d'Alembert's Paradox* [6, 7, 8, 9, 15] comparing observations of substantial drag/lift of a body moving through a slightly viscous fluid such as air and water, with the mathematical prediction of zero drag/lift of stationary irrotational solutions of the incompressible inviscid Euler equations, referred to as *potential flow*. We present analytical and computational evidence that (i) potential flow cannot be observed because it is *illposed* or unstable to perturbations, (ii) computed viscosity solutions of the Euler equations [11] with *slip* boundary conditions initiated as potential flow develop into *turbulent solutions*, which are *wellposed* with respect to drag/lift and show substantial drag/lift. Additional evidence is presented in [25] and the related work on

*Computer Science and Communication, KTH, SE-10044 Stockholm, Sweden.

blowup of Euler solutions [28], separation in inviscid flow [27], and drag/lift of airplanes and cars [30, 29].

D'Alembert was led to formulate his paradox as follows working on a 1749 Prize Problem of the Berlin Academy on flow drag [7]:

> *It seems to me that the theory (potential flow), developed in all possible rigor, gives, at least in several cases, a strictly vanishing resistance, a singular paradox which I leave to future Geometers to elucidate.*

Euler had come to same conclusion of zero drag of potential flow in his work on gunnery [10] from 1745 based on the observation that in potential flow the high pressure forming in front of the body is balanced by an equally high pressure in the back, in the case of a boat moving through water expressed as

> *...the boat would be slowed down at the prow as much as it would be pushed at the poop...*

The commonly accepted resolution of d'Alembert's Paradox propagated in the fluid dynamics literature is attributed to Ludwig Prandtl, called the father of modern fluid mechanics, who in the short note *On the motion of fluids with very small viscosity* [32] from 1904, suggested that drag/lift possibly could emanate from a *no-slip* boundary condition with the tangential velocity changing from a non-zero free-stream value to zero in a thin viscous boundary layer generating *transversal vorticity* and thereby changing the global flow. Prandtl was inspired by Saint-Venant stating in 1846 [33]:

> *But one finds another result (non-zero drag) if, instead of an inviscid fluid – object of the calculations of the geometers Euler of the last century – one uses a real fluid, composed of a finite number of molecules and exerting in its state of motion unequal pressure forces having components tangential to the surface elements through which they act; components to which we refer as the friction of the fluid, a name which has been given to them since Descartes and Newton until Venturi.*

Saint-Venant and Prandtl thus suggested that drag in a real fluid possibly could result from tangential frictional forces in a thin viscous boundary layer creating transversal vorticity, and accordingly inviscid potential flow could be discarded because it has no boundary layer. These suggestions have over time been transformed to become an accepted fact of modern fluid dynamics, questioned by few. Birkhoff conjectured in [1] that drag instead could be the result of an instability of potential flow, but after a devastating review [35] did not pursue this line of thought.

We find by computational solution of the Euler equations with slip boundary conditions, that the potential solution develops into a turbulent solution with substantial drag/lift resulting from streaks of low-pressure *streamwise vorticity* generated from an instability of potential flow at rear separation. We thus obtain without any presence of viscous boundary layers, substantial drag/lift in accordance with observations and the conjecture of Birkhoff.

We motivate the slip boundary condition by benchmark computations and observations indicating that the *skin friction* decreases to zero with the viscosity [34]. These facts are in direct contradiction to Prandtl's claim that effects of skin friction on drag/lift remain substantial under vanishing viscosity.

In particular, we show in [29, 30] that drag/lift of a car or airplane can be accurately predicted by computing turbulent solutions of the Euler equations with slip boundary conditions without resolving thin boundary layers. This is by fluid dynamics expertize considered to be impossible with the motivation that thin boundary layers have to be computationally resolved to correctly capture drag/lift, which for an airplane would require 10^{16} mesh points [19] and is beyond the capacity of any foreseeable computer. Our resolution of d'Alembert's paradox thus seems to offer new possibilities in computational fluid dynamics: Computational solution of the Euler equations can provide a wealth of information in line with the expectations of Euler, after an incubation period of 250 years.

To solve the Euler equations computationaly we use an adaptive finite element method referred to as EG2 with a duality-based a posteriori error control of drag/lift presented in detail in [25, 20, 21, 23, 24], and in executable form available from the Unicorn-project under FEniCS [37], allowing direct verification of the computational results of this note.

An outline is as follows: We first recall the notion of wellposedness and the Euler equations for inviscid incompressible fluid flow together with the potential solution with zero drag for flow around a circular cylinder. We analyze the stability of the potential solution and find different perturbation growth in the front and back of the cylinder causing a pressure drop in the back resulting in drag. We then introduce the concepts of viscosity solution, turbulent solution and EG2 solution and present computational evidence of wellposedness of drag/lift of turbulent EG2 solutions, including the drag of a car (in direct contradiction to state of the art CFD). We then summarize the evidence of our resolution of d'Alembert's paradox and compare with Prandtl's resolution.

2 Wellposedness

Since Hadamard [14] it is well understood that solving differential equations, such as the Euler equations, perturbations of data have to be taken into account. If a vanishingly small perturbation can have a major effect on a solution, then the solution is *illposed*, and in this case the solution may not carry any meaningful information and thus may be meaningless from both mathematical and applications points of view. According to Hadamard, only a *wellposed*

solution, for which small perturbations have small effects on certain solution *outputs*, can be meaningful.

We shall present evidence that a potential solution is illposed with respect to all outputs, including drag/lift, and thus explain why the zero-drag prediction of potential flow carries no information. We also present evidence that computed turbulent EG2 solutions are wellposed with respect to drag/lift and thus can give valuable information. Although wellposedness in the form of hydrodynamic stability is a key issue in fluid dynamics literature, a stability analysis of potential solutions seems to be lacking.

3 The Incompressible Euler Equations

We recall the Euler equations expressing conservation of momentum and mass of an incompressible inviscid fluid enclosed in an open set Ω in $\mathbb{R}^3$ with boundary Γ: Find the velocity $u = (u_1, u_2, u_3)$ and pressure p depending on $(x, t) \in \Omega \cup \Gamma \times I$ such that

$$\begin{aligned} \dot{u} + (u \cdot \nabla)u + \nabla p &= f && \text{in } \Omega \times I, \\ \nabla \cdot u &= 0 && \text{in } \Omega \times I, \\ u \cdot n &= g && \text{on } \Gamma \times I, \\ u(\cdot, 0) &= u^0 && \text{in } \Omega, \end{aligned} \tag{1}$$

where n denotes the outward unit normal to Γ, f is a given volume force, g is a given inflow/outflow velocity, u^0 is a given initial condition, $\dot{u} = \frac{\partial u}{\partial t}$ and $I = [0, T]$ a given time interval. We notice the *slip boundary condition* expressing inflow/outflow with zero friction with $g = 0$ at a solid boundary.

4 Exponential Instability of Linearized Equations

The lack of viscosity with regularizing effect make the Euler equations inaccessible to an analytical mathematical study. The difficulty is exposed by formal linearization: Subtracting the Euler equations for two solutions (u, p) and $(\bar{u}, \bar{p})$ with corresponding (slightly) different data, we obtain the following linearized equation for the difference $(v, q) \equiv (u - \bar{u}, p - \bar{p})$:

$$\begin{aligned} \dot{v} + (u \cdot \nabla)v + (v \cdot \nabla)\bar{u} + \nabla q &= f - \bar{f} && \text{in } \Omega \times I, \\ \nabla \cdot v &= 0 && \text{in } \Omega \times I, \\ v \cdot n &= g - \bar{g} && \text{on } \Gamma \times I, \\ v(\cdot, 0) &= u^0 - \bar{u}^0 && \text{in } \Omega. \end{aligned} \tag{2}$$

Formally, with u and $\bar{u}$ given, this is a linear convection-reaction problem for (v, q) with the reaction term given by the 3×3 matrix $\nabla\bar{u}$. By the incompressiblity, the trace of $\nabla\bar{u}$ is zero, which shows that in general $\nabla\bar{u}$ has eigenvalues with real value of both signs, of the size of $|\nabla\bar{u}|$ (with $|\cdot|$ some matrix norm), thus with at least one exponentially unstable eigenvalue.

Accordingly, we expect local exponential perturbation growth of size $\exp(|\nabla u|t)$ of a solution (u, p), in particular we expect a potential solution to be illposed.

This is seen in EG2 solutions initiated as potential flow, which subject to residual perturbations of mesh size h, in $\log(1/h)$ time develop into turbulent solutions. We give computational evidence that these turbulent solutions are wellposed, which we rationalize by cancellation effects in the linearized problem, which has rapidly oscillating coefficients when linearized at a turbulent solution.

Formally applying the curl operator $\nabla\times$ to the momentum equation of (1) we obtain the vorticity equation

$$\dot{\omega} + (u\cdot\nabla)\omega - (\omega\cdot\nabla)u = \nabla\times f \quad \text{in } \Omega, \tag{3}$$

which is a convection-reaction equation in the vorticity $\omega = \nabla\times u$ with coefficients depending on u, of the same form as the linearized equation (2), with similar properties of exponential perturbation growth $\exp(|\nabla u|t)$ referred to as *vortex stretching*. It is often argued that from the vorticity equation (3), it follows that vorticity cannot be generated starting from potential flow with zero vorticity and $f = 0$, which is *Kelvin's theorem*. But this is an incorrect conclusion, since perturbations $\bar{f}$ of f with $\nabla\times\bar{f}\neq 0$ must be taken into account and the perturbation growth $\exp(|\nabla u|t)$ is very large if only the exponent is moderatly large. What we see in EG2 computations of the cylinder flow, is local exponential growth of vorticity by vortex stretching at rear separation, which is a main route in the transition to turbulence.

5 Viscous Regularization

We define the *Euler residual* by

$$R(u,p) \equiv \dot{u} + (u\cdot\nabla)u + \nabla p - f, \tag{4}$$

which is the residual of the momentum equation, assuming for simplicity that the incompressiblity equation $\nabla\cdot u = 0$ is not subject to perturbations. *The regularized Euler equations* take the form: Find (u_ν, p_ν) such that

$$\begin{array}{rcll} R(u_\nu,p_\nu) & = & -\nabla\cdot(\nu\nabla u_\nu) & \text{in } \Omega\times I,\\ \nabla\cdot u_\nu & = & 0 & \text{in } \Omega\times I,\\ u_\nu\cdot n & = & g & \text{on } \Gamma\times I,\\ u_\nu(\cdot,0) & = & u^0 & \text{in } \Omega, \end{array} \tag{5}$$

where $\nu > 0$ is a small *viscosity*, together with a homogeneous Neumann boundary condition for the tangential velocity. Notice that we keep the slip boundary condition $u_\nu\cdot n = g$, which eliminates viscous no-slip boundary layers, and the turbulence we will discover thus does not emanate from boundary layers with tangential skin friction. We consider here a standard regularization and present EG2 regularization in the next section. Existence of a pointwise solution (u_ν, p_ν) of (5) (allowing ν to have a certain dependence on $|\nabla u|$), follows by standard techniques, see e.g. [3]. Notice that the Euler residual $R(u_\nu, p_\nu)$ equals the viscous term $-\nabla\cdot(\nu\nabla u_\nu)$, which suggests an interpretation of the viscous term in the form of the Euler residual.

The standard *energy estimate* for (5) is obtained by multiplying the momentum equation with u_ν and integrating in space and time, to get in the case $f = 0$ and $g = 0$,

$$\int_0^t \int_\Omega R(u_\nu, p_\nu) \cdot u_\nu \, dxdt = D(u_\nu; t) \equiv \int_0^t \int_\Omega \nu |\nabla u_\nu(s, x)|^2 dxds, \tag{6}$$

from which follows by standard manipulations of the left hand side,

$$K(u_\nu(t)) + D(u_\nu; t) = K(u^0), \quad t > 0, \tag{7}$$

where

$$K(u_\nu(t)) = \frac{1}{2} \int_\Omega |u_\nu(t, x)|^2 dx.$$

This estimate shows a balance of the *kinetic energy* $K(u_\nu(t))$ and the *viscous dissipation* $D(u_\nu; t)$, with any loss in kinetic energy appearing as viscous dissipation, and vice versa. In particular $D(u_\nu; t) \leq K(0)$ and thus the viscous dissipation is bounded (if $f = 0$ and $g = 0$).

Turbulent solutions of (5) are characterized by *substantial turbulent dissipation*, that is (for t bounded away from zero),

$$D(t) \equiv \lim_{\nu \to 0} D(u_\nu; t) >> 0. \tag{8}$$

That a positive limit (~ 1) exists is *Kolmogorov's conjecture*, which is consistent with

$$\|\nabla u_\nu\|_0 \sim \frac{1}{\sqrt{\nu}}, \quad \|R(u_\nu, p_\nu)\|_0 \sim \frac{1}{\sqrt{\nu}}, \tag{9}$$

where $\|\cdot\|_0$ denotes the $L_2(Q)$-norm with $Q = \Omega \times I$. On the other hand, it follows by standard arguments from (7) that

$$\|R(u_\nu, p_\nu)\|_{-1} \leq \sqrt{\nu}, \tag{10}$$

where $\|\cdot\|_{-1}$ is the norm in $L_2(I; H^{-1}(\Omega))$. Kolmogorov thus conjectures that the Euler residual $R(u_\nu, p_\nu)$ is strongly (in L_2) large, while being small weakly (in H^{-1}).

6 EG2 Regularization

An EG2 solution (U, P) on a mesh with local mesh size $h(x, t)$ according to [25], satisfies the following energy estimate (with $f = 0$ and $g = 0$):

$$K(U(t)) + D_h(U; t) = K(u^0), \tag{11}$$

where

$$D_h(U; t) = \int_0^t \int_\Omega hR(U, P)^2 \, dxdt, \tag{12}$$

is an analog of $D(u_\nu;t)$ with $h \sim \nu$. We see that the EG2 viscosity arises from penalization of a non-zero Euler residual $R(U,P)$ with the penalty directly connecting to the violation (according the theory of criminology). A turbulent solution is characterized by substantial dissipation $D_h(U;t)$ with $\|R(U,P)\|_0 \sim h^{-1/2}$, and

$$\|R(U,P)\|_{-1} \leq \sqrt{h} \tag{13}$$

in accordance with (9) and (10).

EG2 explains the occurence of viscous effects in Euler solutions in a new way, not simply assuming ad hoc that "there is always some small constant shear viscosity", but from the *impossibility of pointwise exact conservation of momentum*. EG2 viscosity is not a simple constant shear viscosity but rather a solution dependent bulk (or streamline) viscosity [25, 26].

7 Wellposedness of Mean-Value Outputs

Let $M(v) = \int_Q v \cdot \psi \; dxdt$ be a *mean-value output* of a velocity v defined by a smooth weight-function $\psi(x,t)$, and let (u,p) and (U,P) be two EG2-solutions on two meshes with maximal mesh size h. Let (φ,θ) be the solution to the *dual linearized problem*

$$\begin{array}{rcll} -\dot{\varphi} - (u\cdot\nabla)\varphi + \nabla U^\top\varphi + \nabla\theta &=& \psi & \text{in } \Omega\times I,\\ \nabla\cdot\varphi &=& 0 & \text{in } \Omega\times I,\\ \varphi\cdot n &=& g & \text{on } \Gamma\times I,\\ \varphi(\cdot,T) &=& 0 & \text{in } \Omega, \end{array} \tag{14}$$

where $\top$ denotes transpose. Multiplying the first equation by $u-U$ and integrating by parts, we obtain the following output error representation [25, 26]:

$$M(u) - M(U) = \int_Q (R(u,p) - R(U,P))\cdot\varphi \, dxdt \tag{15}$$

from which follows the a posteriori error estimate

$$|M(u) - M(U)| \leq S(\|R(u,p)\|_{-1} + \|R(U,P)\|_{-1}), \tag{16}$$

expressing wellposedness of the output $M(\cdot)$ with respect to residual perturbations, where the stability factor

$$S = S(u,U,M) = S(u,U) = \|\varphi\|_{H^1(Q)}. \tag{17}$$

In [25] we present a variety of evidence, obtained by computational solution of the dual problem, that for global mean-value outputs such as drag and lift, $S << 1/\sqrt{h}$, while $\|R\|_{-1} \sim \sqrt{h}$, allowing computation of of drag/lift with a posteriori error control within one or a few percent.

8 Stability of the Dual Linearized Problem

A crude analytical stability analysis of the dual linearized problem (14) using Gronwall type estimates, indicates that the dual problem is pointwise exponentially unstable because the reaction coefficient ∇U is locally very large. This is consistent with massive observation that point-values of turbulent flow are non-unique or unstable.

On the other hand we observe computationally that S is of moderate size for mean-value outputs of turbulent solutions. We explain in [25] this remarkable fact as an effect of *cancellation* from the following two sources:

(i) rapidly oscillating reaction coefficients of turbulent solutions,

(ii) smooth data in the dual problem for mean-value outputs.

For a laminar potential solution there is no cancellation, and therefore not even mean-values are wellposed.

9 Potential Flow around a Circular Cylinder

We consider potential flow (stationary irrotational flow) around an cylinder of diameter 1 oriented along the x_3-axis and immersed in an inviscid incompressible fluid filling $\mathbb{R}^3$ with velocity $(1,0,0)$ at infinity. The potential velocity is given as $u = \nabla\phi$, where ϕ satisfies Laplace's equation $\Delta\phi = 0$ outside the cylinder with $\nabla\phi = (1,0,0)$ at infinity and accordingly is given by

$$\phi(x_1,x_2,x_3) = (r + \frac{1}{r})\cos(\theta), \tag{18}$$

where $(x_1,x_2) = (r\cos(\theta), r\sin(\theta))$ is expressed in polar coordinates (r,θ). In Fig. 1 we plot the streamlines of u in a section of the cylinder, which are the curves followed by fluid particles, and the pressure. We notice that the potential flow (in each section) has one *separation point* at the back of the cylinder, where the flow separates from the cylinder boundary. We also notice that the both velocity and pressure are symmetric in the flow direction (x_1-direction), which means that the drag of the cylinder is zero, as noted by Euler and d'Alembert: the pressure in front of the cylinder is balanced by the same pressure behind, in contradiction to observations of lower pressure in the back with corresponding substantial drag.

10 EG2 Solution of Cylinder Flow

We compute by EG2 the flow around a circular cylinder in a channel with given inflow velocity $(1,0,0)$ choosing the initial velocity $u^0 = 0$. We see the zero-drag irrotational potential solution quickly developing during the first time steps, but the potential solution gradually changes into a turbulent solution with substantial drag and vorticity and a low pressure wake, see Fig. 2. We observe

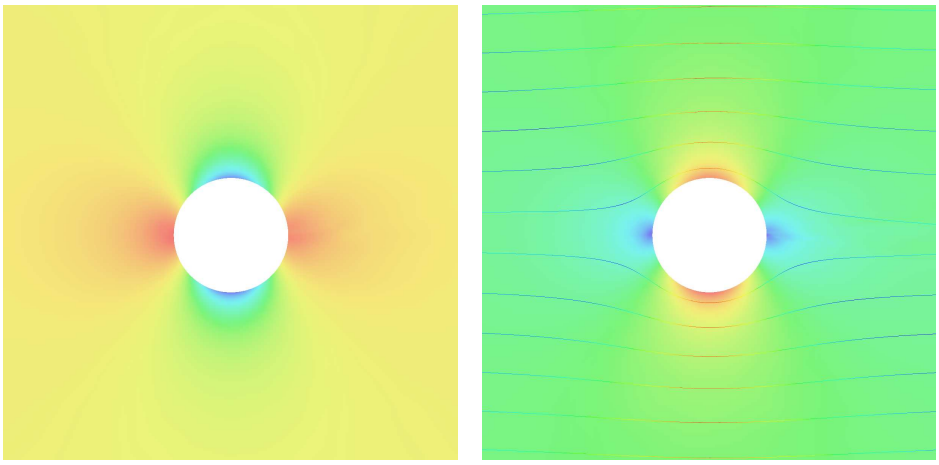

Figure 1: Potential solution of the Euler equations for flow past a circular cylinder; colormap of the pressure (left) and streamlines together with a colormap of the magnitude of the velocity (right) .

the following key features of EG2 solutions, which are not features of Prandtl's resolution: (a) no boundary layer prior to separation, (b) one separation point in each section of the cylinder which oscillates up and down and (c) strong vorticity in the streamwise direction in the wake. The computed drag coefficient $c_D \approx 1.0$, which is consistent under mesh refinement, and which fits with the observation [36] that the drag increases from ≈ 0.5 to about 1.0 beyond the drag crisis occuring for a Renolds number $\approx 10^6$. We see that the solution looks very similar to the experiments of Prandtl [32], see Fig. 3, and in Fig. 4 we see that the streamwise (x_1) vorticity dominates the tranversal (x_3) vorticity, and that the pressure is low inside tubes of vorticity in the x_1-direction behind the cylinder, which creates drag.

11 Stability Analysis of Potential Flow

We shall now in a more precise model analysis of the linearized equations, motivate the development of the low pressure streaks of streamwise vorticity attaching at rear separation, which cause the drag, as a result of different perturbation growth at forward attachment and rear separation.

We start approximating the potential flow at rear separation by $u = (x_1, -x_2, 0)$ by replacing the cylinder by the half-plane $\{x_1 > 0\}$ as in Fig. 5. Assuming x_1 and x_2 are small, we can approximate the v_2-equation of (2) by

$$\dot{v}_2 - v_2 = f_2,$$

where $f_2 = f_2(x_3)$ is an oscillating mesh residual perturbation depending on x_3 (including also a pressure-gradient), for example $f_2(x_3) = h\sin(x_3/\delta)$, with

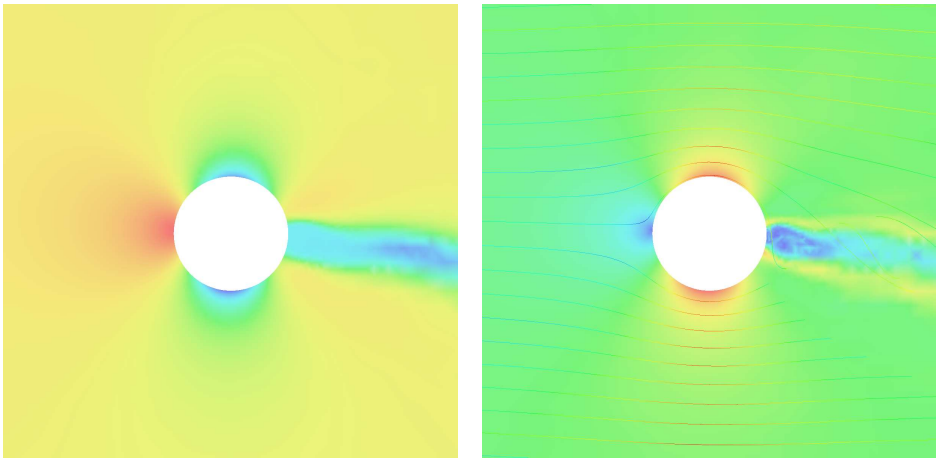

Figure 2: Computational solution of the Euler equations for flow past a circular cylinder; colormap of the pressure (left) and streamlines together with a colormap of the magnitude of the velocity (right) .

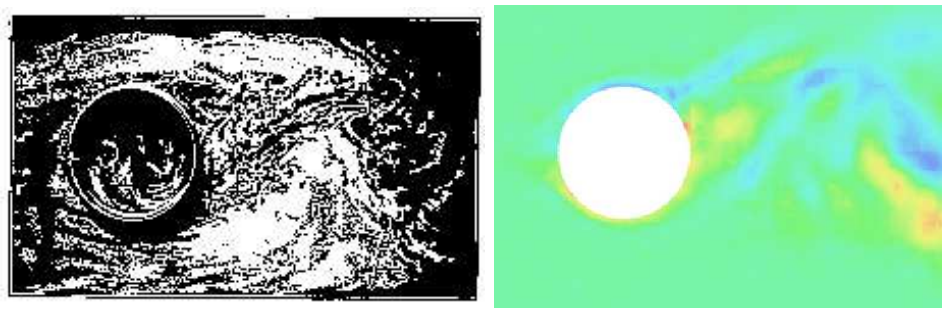

Figure 3: Vorticity in turbulent flow past a circular cylinder: Prandtl's experiment (left), and a computational solution without boundary layer (right).

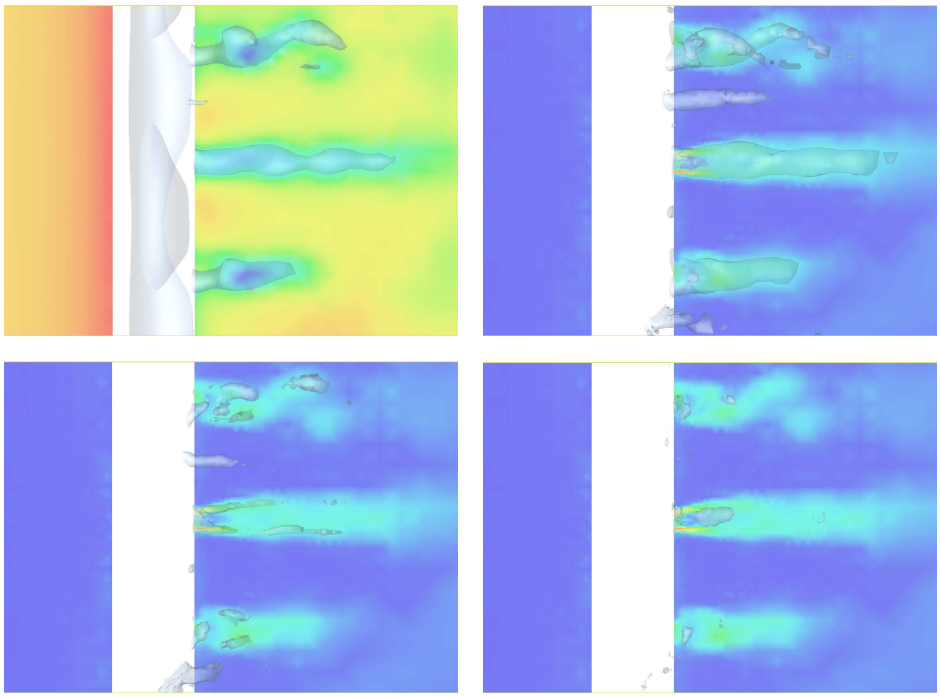

Figure 4: Computational solution of the Euler equations for flow past a circular cylinder; colormap of the pressure and isosurfaces for low pressure (upper left), colormap of the magnitude of total vorticity and isosurfaces for high magnitude of the individual components: x_1-vorticity (upper right), x_2-vorticity (lower left), x_3-vorticity (lower right).

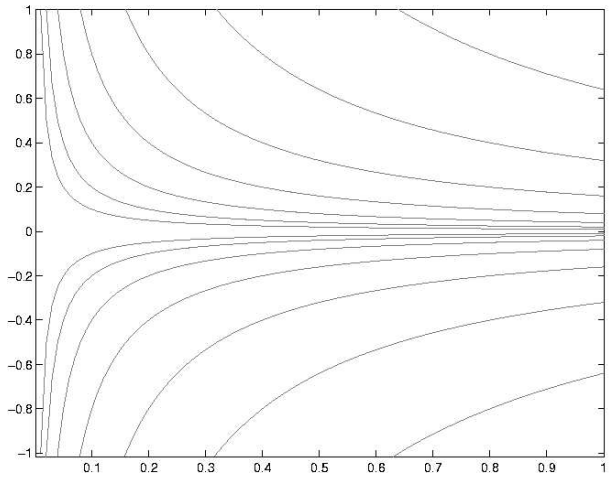

Figure 5: Model of potential solution at rear separation.

$\delta > 0$. It is natural to assume that the amplitude of f_2 decreases with δ. We conclude, assuming $v_2(0,x) = 0$, that

$$v_2(t,x_3) = t\exp(t)f_2(x_3),$$

and for the discussion, we assume $v_3 = 0$. Next we approximate the ω_1-vorticity equation in (3) for x_2 small and $x_1 \geq \bar{x}_1 > 0$ with $\bar{x}_1$ small, by

$$\dot{\omega}_1 + x_1\frac{\partial \omega_1}{\partial x_1} - \omega_1 = 0,$$

with the "inflow boundary condition"

$$\omega_1(\bar{x}_1,x_2,x_3) = \frac{\partial v_2}{\partial x_3} = t\exp(t)\frac{\partial f_2}{\partial x_3}.$$

The equation for ω_1 thus exhibits exponential growth, which is combined with exponential growth of the "inflow condition". Altogether we expect $\exp(t)$ perturbation growth of residual perturbations of size h, resulting in a global change of the flow after time $T \sim \log(1/h)$, which can be traced in the computations. Since the combined exponential growth is independent of δ, it follows that a large-scale perturbations with large amplitude have largest growth. This is seen in computations, where δ is of the size of the diameter of the cylinder.

We can thus understand the formation of streamwise streaks of vorticity at rear separation as the result of a force perturbation oscillating in the x_3 direction, which by the retardation in the x_2-direction creates vorticity in the x_1-direction, which is further magnified by vortex stretching. Thus, we find exponential perturbation growth at rear separation from both the retardation in the x_2-direction and the accelleration in the x_1 direction.

We next model the attaching flow at the front by $u = (-x_1,x_2)$ in the half-plane $x_1 < 0$. In this case, u_1 is retarding before attachment, but not by meeting an opposing flow as u_2 does at separation, which means that the analog of the perturbation f_2, cannot be established in attachment at the front. After attachment, the flow is accelerating in the x_2 direction with corresponding exponential growth of ω_2, but in this case without the inflow occuring at rear separation. The presence of small ω_2-vorticity at the leading edge of an airfoil is visible e.g. in Fig. 1.15 of [25].

12 EG2 solution of a car

We note that the resolution of the paradox without the need for a boundary layer has important practical implications, as the common pessimistic predictions for high Reynolds number computational fluid mechanics [19] are based on the computational cost of resolving turbulent boundary layers. On the other hand, a resolution of the paradox without boundary layers open for a wealth of advanced computations, previously deemed impossible. In particular, in Fig. 6 we show a computation of the turbulent flow around a car using EG2, presented in detail in [29], with separation and drag consistent with what we expect from experiments.

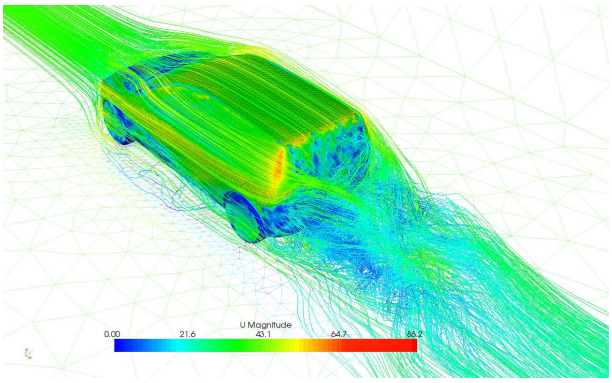

Figure 6: EG2 solution of the turbulent flow around a car (geometry courtesy of Volvo Car Corporation).

13 Summary

We have presented a resolution of d'Alembert's Paradox based on analytical and computational evidence that a potential solution with zero drag is illposed as a solution of the Euler equations, and under perturbations develops into a well-posed turbulent solution with substantial drag in accordance with observations.

Our resolution is fundamentally different from that proposed by Saint Venant and Prandtl suggesting that drag/lift can emanate from viscous boundary layers even with vanishingly small viscosity. We have presented evidence that correct drag/lift can be obtained by computing turbulent solutions of the Euler equations with slip boundary conditions. We have thus shown that drag/lift mainly results from the turbulent nature of the flow and only to a small part from viscous boundary layers.

Acknowledgements

The first author would like to acknowledge the financial support of the Swedish Foundation for Strategic Research. The authors would also like to thank Murtazo Nazarov for carrying out the EG2 computations of the car.

References

[1] Garret Birkhoff, *Hydrodynamics: a study in logic, fact and similitude*, Princeton University Press, 1950.

[2] Sergei Chernyshenko, Peter Constantin, James Robinson and Endriss Titi, A posteriori regularity of the three-dimensional Navier-Stokes equations from computations.

[3] Peter Constantin, Euler equations, Navier-Stokes Equations and Turbulence, CIME Lecture Notes, 2003.

[4] Peter Constantin, On the Euler Equations of Incompressible Fluids, Bull. Amer. math. Soc. 44 (2007), 603-21.

[5] O. Darrigol, World of Flow, A History of hydrodynamics from the Bernouillis to Prandtl, Oxford University Press.

[6] Jean le Rond d'Alembert, Theoria resistentiae quam patitur corpus in fluido motum, ex principiis omnino novis et simplissimus deducta, habita ratione tum velocitatis, figurae, et massae corporis moti, tum densitatis compressionis partium fluidi; Berlin-Brandenburgische Akademie der Wissenschaften, Akademie-Archiv call number: I-M478, 1749.

[7] Jean le Rond d'Alembert, Essai d'une nouvelle théorie de la résistance des fluides, Paris, 1752.

[8] Jean le Rond d'Alembert, Paradoxe proposé aux géomètres sur la résistance des fluides, in Opuscules mathématiques, Vol 5, Memoir XXXIV, I, 132-138, 1768.

[9] Jean le Rond d'Alembert, Sur la Résistance des fluides, in Opuscules mathématiques, Vol 8, Memoir LVII, 13, 210-230, 1780.

[10] Leonard Euler, Neue Grundsäteze der Artillerie, Berlin, 1745.

[11] Leonard Euler, Principes généraux du mouvement des fluides, Académie Royale des Sciences et des Belles-Lettres de Berlin, Mémoires 11, 274-315, 1755.

[12] Leonard Euler, Delucidationes de resistentia fluidorum, Novi Commenatrii academiae scientiarum imperialis Petropolitanae, 8, 1756.

[13] Charles Fefferman, Existence and Smoothness of the Navier-Stokes Equations, Official Clay Mathematics Institute Millenium Problem for the Navier-Stokes equations.

[14] Jacques Hadamard, Sur les problmes aux dérivées partielles et leur signification physique. Princeton University Bulletin, 49-52, 1902.

[15] G. Grimberg, W. Pauls and U. Frisch, Genesis of d'Alembert's paradox and analytical elaboration of the drag problem, Physica D, to appear.

[16] J. Deng, T. Y. Hou, and X. Yu, Geometric properties and the non-blowup of the three-dimensional Euler equation, Comm. PDEs, 30:1 (2005), 225-243.

[17] J. Deng, T. Y. Hou, and X. Yu, Improved Geometric Conditions for Non-blowup of the 3D Incompressible Euler Equation, Communication in Partial Differential Equations, 31 (2006), 293-306.

[18] T. Y. Hou and R. Li, Dynamic Depletion of Vortex Stretching and Non-Blowup of the 3-D Incompressible Euler Equations, J. Nonlinear Science, 16 (2006), 639-664.

[19] P. Moin and J. Kim, Tackling Turbulence with Supercomputers, Scientific Ameican, 1997.

[20] Johan Hoffman. Computation of mean drag for bluff body problems using adaptive dns/les. *SIAM J. Sci. Comput.*, 27(1):184–207, 2005.

[21] Johan Hoffman. Adaptive simulation of the turbulent flow past a sphere. *J. Fluid Mech.*, 568:77–88, 2006.

[22] Johan Hoffman. Computation of turbulent flow past bluff bodies using adaptive general galerkin methods: drag crisis and turbulent euler solutions. *Comput. Mech.*, 38:390–402, 2006.

[23] Johan Hoffman. Efficient computation of mean drag for the subcritical flow past a circular cylinder using general galerkin g2. *Int. J. Numer. Meth. Fluids*, accepted.

[24] Johan Hoffman and Claes Johnson. A new approach to computational turbulence modeling. *Comput. Methods Appl. Mech. Engrg.*, 195:2865–2880, 2006.

[25] J. Hoffman and C. Johnson, *Computational Turbulent Incompressible Flow*, Springer, 2007.

[26] J. Hoffman and C. Johnson, *Computational Thermodynamics*, Springer, 2008.

[27] J. Hoffman and C. Johnson, Flow separation at large Reynolds numbers, in preparation.

[28] J. Hoffman and C. Johnson, Blowup of incompressible Euler solutions, to appear in BIT Numerical Mathematics.

[29] J. Hoffman, J. Jansson, N. Jansson and M. Nazarov, Computational simulation of the turbulent flow past a car using a General Galerkin method, in preparation.

[30] J. Hoffman, J. Jansson, N. Jansson and M. Nazarov, Computational simulation of the turbulent flow past an airplane using a General Galerkin method, in preparation.

[31] G. Ponce, Remarks on a paper by J.T. Beale, T. Kato and A. Majda, Commun. Math. Phys. 98, 349-352, 1985.

[32] L. Prandtl. On motion of fluids with very little viscosity. *Third International Congress of Mathematics, Heidelberg, http://naca.larc.nasa.gov/digidoc/report/tm/52/NACA-TM-452.PDF*, 1904.

[33] A. Saint-Venant, Résistance des fluides: considérations historiques, physiques et pratiques relatives au problème de l'action dynamique mutuelle d'un fluide a d'un solide, dans l'état de permanence supposé acquis par leurs mouvements, Academie des Science, Mémoires 44, 1-280.

[34] H. Schlichting, Boundary Layer Theory, McGraw-Hill, 1955.

[35] J. Stoker, Bull. Amer. Math. Soc. Am. Math., Vol 57(6), pp 497-99.

[36] D. J. Tritton. *Physical Fluid Dynamics*. 2nd ed. Oxford, Clarendon Press, 1988.

[37] FEniCS. Fenics project. *http://www.fenics.org*, 2003.